

The application of a VUV Fourier transform spectrometer and synchrotron radiation source to measurements of: I. The $\beta(9,0)$ band of NO

K. Yoshino,^{a)} J. R. Esmond, and W. H. Parkinson
Harvard-Smithsonian Center for Astrophysics, Cambridge, Massachusetts 02138

A. P. Thorne, J. E. Murray, R. C. M. Learner, and G. Cox
Blackett Laboratory, Imperial College, London, SW7-2BZ, United Kingdom

A. S.-C. Cheung and K. W.-S. Leung
The University of Hong Kong, Hong Kong

K. Ito and T. Matsui^{b)}
Photon Factory, KEK, Tsukuba, Ibaraki 305, Japan

T. Imajo
Kyushu University, Fukuoka 812, Japan

(Received 5 March 1998; accepted 22 April 1998)

State-of-the-art models of the vacuum ultraviolet (VUV) absorbing properties of the atmosphere call for absorption cross sections with detail on the scale of the Doppler widths. As a consequence, spectroscopic data at resolving powers of the order of 10^6 are needed. To meet these requirements in the vacuum ultraviolet region, we have used the VUV Fourier transform spectrometer from Imperial College, London, at the synchrotron radiation facility at Photon Factory, KEK, Japan, to measure photoabsorption cross sections of NO from 195 to 160 nm, and of O₂ from 185 to 175 nm. The analysis of the $\beta(9,0)$ band ($B^2\Pi_r-X^2\Pi_r$) of NO provides accurate rotational line positions and term values. Molecular constants of the $B(9)^2\Pi$ level are $T_0 = 54\,205.097 \pm 0.012$ cm⁻¹, $A = 45.320 \pm 0.021$ cm⁻¹, $B_v = 1.016\,72 \pm 0.000\,16$ cm⁻¹, $D_v = (10.61 \pm 0.32) \times 10^{-6}$ cm⁻¹, and $A_D = 0.001\,22 \pm 0.000\,11$ cm⁻¹. The rotational line strengths and the branching ratios are also presented. The band oscillator strength is obtained as $f = 2.65 \times 10^{-4}$. © 1998 American Institute of Physics. [S0021-9606(98)01529-3]

I. INTRODUCTION

The molecular absorption processes and parameters related to the absorption of ultraviolet solar radiation in the terrestrial middle atmosphere have been discussed by a number of authors.¹⁻⁴ In the spectral region 175–205 nm, the penetration of solar radiation into the atmosphere is controlled by the absorption cross sections of the Schumann–Runge (S-R) bands of O₂. Part of the radiation transmitted in this vacuum ultraviolet (VUV) wavelength region is available to photodissociate NO, which has a number of strong bands there with very narrow lines.^{5,6} For accurate modeling of this important process, the computations involving O₂ and NO must be performed on a line-by-line basis; laboratory-measured photoabsorption cross sections, with resolution sufficient to yield true cross sections (i.e., undegraded by instrumental effects), are required for both molecules. For most of the S-R bands of ¹⁶O₂ and its important isotopic variants, such measurements have been successfully completed at the Center for Astrophysics.⁷⁻⁹

In order to improve further our understanding of the important NO photodestruction process,¹⁰⁻¹⁴ similar measurements of band oscillator strengths and predissociation linewidths of some band systems of NO are needed. Hart and

Bourne¹⁵ have reported much larger linewidths for the $\delta(1,0)$ band than those by Frederick and Hudson.¹¹ Such differences and uncertainties in the oscillator strengths and predissociation widths have been found to have a significant impact on the uncertainties of the effects of NO opacity and, consequently, on the photolysis rate.¹⁴

Until our recent work,¹⁶ all previous quantitative photoabsorption measurements of these NO bands¹⁷⁻¹⁹ have been performed at insufficient spectroscopic resolution. Published integrated cross sections in some cases differ by more than 50%; the differences could indicate that some of the measurements were plagued by saturation, which is very difficult to detect when linewidths are much narrower than the instrument widths.²⁰ Because the band oscillator strengths and predissociation linewidths of the bands of NO have not been directly measured with sufficient resolution, line-by-line calculations of the aeronomic dissociation of NO¹² rely on assumptions, of unknown and differing reliability, about possibly problematic molecular data.

We recently used one of the Fourier transform (FT) spectrometers at Imperial College, London, (IC) to measure the absorption cross sections of the $\delta(0,0)$ and $\beta(7,0)$ bands of NO in the region 195–183 nm with a resolution of 0.06 cm⁻¹.¹⁶ A positive-column hydrogen-discharge at high current (~ 500 mA) was used for a background continuum, with a stigmatic 0.3 m Czerny–Turner spectrometer

^{a)}Electronic mail: kyoshino@cfa.harvard.edu

^{b)}Present address: HSRC, Hiroshima University, Hiroshima 739, Japan.

(McPherson model 218) to limit the bandwidth from 1 to 2 nm. A signal-to-noise (S/N) ratio of 25 was achieved by co-adding up to 128 runs.

Based on these previous experiences, the extension of FT spectrometry (FTS) further into the VUV region requires an efficient spectrometer, a strong and stable continuum source, and a zero dispersion monochromator. This combination was realized by taking the IC VUV FT spectrometer equipped with a beam splitter made from a single crystal of MgF_2 ²¹ to the synchrotron radiation source at Photon Factory, KEK, Japan, where a suitable zero dispersion two-grating predisperser is available on beam line 12-B of the synchrotron radiation source. We have used this combination of facilities to make ultra high resolution cross-section measurements of NO and O_2 bands in the wavelength region 195–160 nm. This paper presents the analysis of the $\beta(9,0)$ ($B^2\Pi_r - X^2\Pi_r$) band of NO.

II. EXPERIMENT

A. VUV FT spectrometers at Imperial College

No Fourier transform spectroscopy had been performed at VUV wavelengths until 1985, when the first laboratory instrument designed specifically for this region was developed and used at Imperial College.²² This VUV FT spectrometer and a commercial version of it manufactured by Chelsea Instruments Ltd. (London), equipped with beam splitters made from fused silica have been used to obtain VUV spectra of emission lines with a resolving power of up to 1.8×10^6 (resolution limit 0.03 cm^{-1}). The FT spectrometers are compact ($l \times w \times h \approx 1.5 \text{ m} \times 0.3 \text{ m} \times 0.3 \text{ m}$) and are designed to be movable. To extend the wavelength range further into the VUV, some improvements were made to the interferometer and a new beam splitter made from a single crystal of MgF_2 ²¹ was installed. This beam splitter was fabricated by B. Halle Nachfl GmbH & Co. (Berlin) to match the fused silica beam splitter and was coated by Acton Research (Acton, MA) for optimum transmission and reflectivity in the VUV. The instrument has been used to record emission spectra down to $\sim 139 \text{ nm}$.

B. The 12-B beam line at the Photon Factory with FT spectrometer

The 12-B beam line of the photon factory has been used with the double grating, zero-dispersion, predisperser and the 6.65 m off-plane Eagle spectrometer.²³ After reflection by the water-cooled, x-ray cutoff, plane mirror (M) radiation from the storage ring hits the first grating (G_1) (see Fig. 1). Radiation of only the desired wavelength region is permitted to pass through the intermediate slit (S_1). The filtered radiation is counter-dispersed by G_2/M_2 onto the main entrance slit (S_2) of the 6.65 m spectrometer, with an approximate image size of $0.1 \times 20 \text{ mm}$.

In our application of the FT spectrometer, a cylindrical mirror (C) was placed right after grating G_2 to reflect radiation by 90° horizontally. The entrance aperture of the FT spectrometer was placed at the position of vertical focus of synchrotron radiation. The cylindrical mirror horizontally focused the radiation to a 2 mm spot at the same place. The

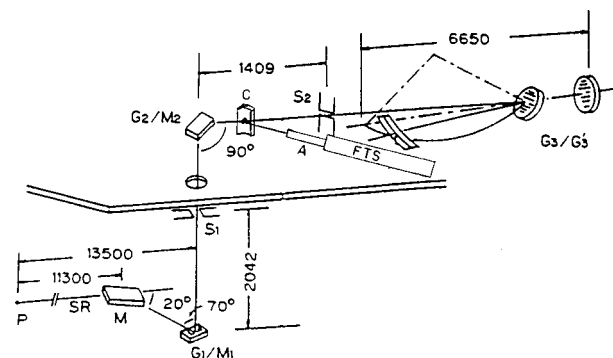


FIG. 1. Optical system of the 6.65 m spectrometer facility (6VOPE) at Photon Factory. A cylindrical mirror (C) is placed right after a grating G_2 to reflect radiation by 90° horizontally into the FT spectrometer (FTS).

entrance aperture was set at 1.5 mm diam for all runs except for the shortest wavelength band, when a 2 mm aperture was used to match the lower resolution used in that run.

The absorption cell (A) was placed between the cylindrical mirror chamber and the FT spectrometer. The optical path lengths could be varied from 0.2 to 8 cm. NO pressure was measured with a capacitance manometer (MKS Baratron) in the range of 0.1 to 1 Torr, corresponding to column densities of 2.9×10^{15} to $2.2 \times 10^{17} \text{ mol cm}^{-2}$. The bandwidth controlled by the predisperser was fixed at 2.0 nm. A total of 18 data files was obtained for NO measurements in the wavelength region 198–160 nm. They are summarized in Table I. S/N ratios of from 30 to 97 in the background continuum were obtained, depending on the spectral region and the number of co-added interferograms—typically, about 300, representing a total integration time of about 14 h.

TABLE I. Conditions of absorption measurements of NO by using VUV FT spectrometer at Photon Factory, Japan. The spectral bandwidth in all cases was 20 Å, the cell temperature was 295 K, and the resolution was 0.06 cm^{-1} for all bands except the shortest wavelength, for which it was 0.12 cm^{-1} .

Band	WL nm	l cm	Pressure Torr	Integrated time hour	S/N
$\gamma(3,0), \beta(6,0)$	198	7.54	0.300	10.7	50
$\delta(0,0), \beta(7,0)$	193	0.565	0.450	11.1	70
$\epsilon(0,0)$	190	0.565	0.300	12.4	97
$\beta(9,0)$	186	7.54	0.400	5.3	57
$\delta(1,0)$	185	0.565	0.200	7.3	66
$\delta(1,0)$	185	0.565	0.400	13.8	96
$\delta(1,0)$	184	0.284	0.314	10.2	80
$\beta(10,0)$	183	7.54	0.900	7.6	63
$\epsilon(1,0)$	181	0.565	0.500	12.7	63
$\beta(11,0)$	180	4.50	0.150	13.5	66
$\beta(12,0), \delta(2,0)$	177	0.565	0.500	12.7	51
$\epsilon(2,0), \beta(13,0)$	174	4.50	0.100	12.4	47
$\beta(14,0)$	173	7.54	0.850	7.6	34
$\beta(14,0)$	173	7.54	0.500	14.9	40
$\delta(3,0)$	170	4.50	0.140	30.6	51
$\epsilon(3,0)$	168	7.54	0.150	13.8	34
$\beta(17,0)$	165	7.54	0.300	14.6	31
$\delta(4,0), \beta(18,0)$	163	7.54	0.170	6.4	33

III. THE $\beta(9,0)$ BAND OF NO

A small amount of NO, purified by the method of fractional distillation, was kept at 78 K in a liquid-nitrogen cooled trap. The NO gas was introduced into the absorption cell at a pressure of 0.40 Torr with an optical path length of 7.54 cm corresponding to a column density of 9.87×10^{16} mol cm^{-2} . In this case we co-added 116 scans, corresponding to about five and a half hours integration time, with spectral resolution of 0.06 cm^{-1} . The S/N ratio in the continuum background was 57.

A. Fitting of the FTS data

The transmission spectra were converted to optical depth by taking the logarithms of the intensity and fitting a smooth continuum to the regions between the lines. The absorption lines were fitted to Voigt profiles using the spectral reduction routine GREMLIN.²⁴ Line parameters are determined through a nonlinear least-squares iterative procedure.

The Voigt profile for the NO lines is a convolution of a Gaussian due to Doppler broadening and a Lorentzian arising from predissociation. In this case the calculated Doppler width is 0.12 cm^{-1} , and the instrumental width for spectra taken at 0.06 cm^{-1} resolution should make a negligible contribution to the overall linewidths. However, the lines proved to be unexpectedly wide, and the Gaussian component of the best fit Voigt function had a (full width at half maximum) FWHM of 0.175 cm^{-1} significantly greater than the 0.12 cm^{-1} expected. Clamping the Doppler width at the expected value gave a worse fit to the line profiles. We do not believe that the anomalous widths can be accounted for by some unexpected (and inherently improbable) degradation of the intrinsic instrumental resolution by a factor of 3 because there is no sign of the ‘ringing’ that should be associated with such significant under-resolution. In the case of the O_2 bands also recorded at photon factory, we have compared our linewidths with those obtained by laser absorption spectroscopy at Australian National University, Canberra and found a similar anomaly.²⁵ We believe the problem may be due to drifts in alignment causing very small wave number shifts over the long observation periods, which were typically double the integration time and extended over two days.

B. Wavelength calibration

As discussed in a previous paper,²⁶ at least one reference wave number is needed for absolute calibration. Mercury vapor was an impurity in the FT spectrometer, and enough was present for the resonance line of Hg I at 184.9 nm to appear in our absorption spectra (see the bottom spectrum of Fig. 2). The structure of this line (a mixture of isotope shifts and hyperfine structure splitting) is not resolved in our spectra. However, the line can be synthesized by combining the absolute wave number of the ^{198}Hg component, $54\,068.9025 \text{ cm}^{-1}$ measured by Kaufman²⁷ with the isotope and hyperfine structure shifts measured by Lecler.²⁸ The synthesized line convolved with the Doppler and instrumental widths, can then be fitted to the measured line to give the required calibration wave number shift. When this procedure was followed with the Hg 253.7 nm line for wave number

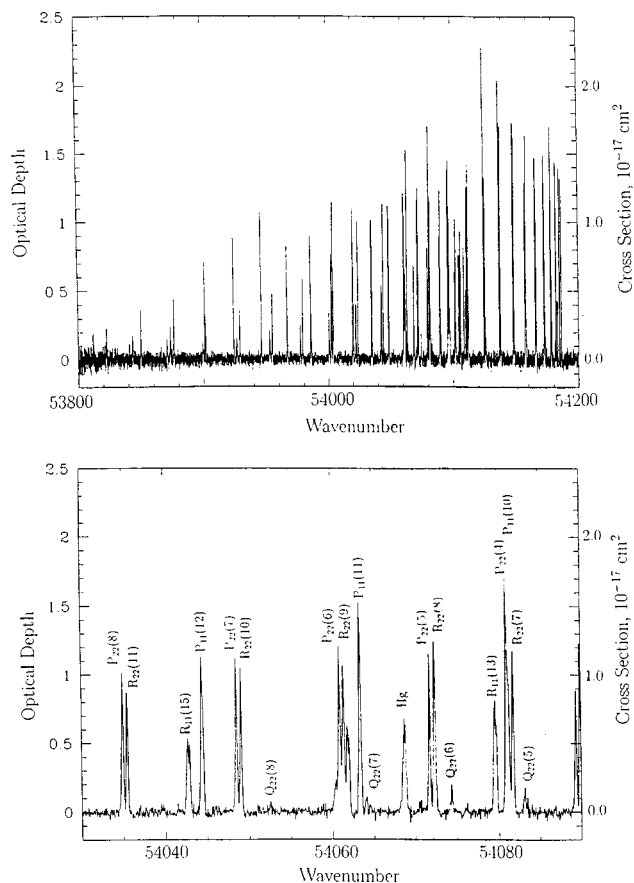


FIG. 2. The $\beta(9,0)$ band at 0.400 Torr of NO with 7.54 cm path length. Rotational assignments are given in term of $J-0.5$, e.g., $P_{22}(8)$ means $P_{22}(8.5)$. Separations by Λ -type doubling are seen in R_{11} branch lines.

calibration of the Herzberg bands,²⁶ the fit of the synthesized and observed profiles was excellent. In the present case the fit is less satisfactory. Nevertheless, the uncertainty in the calibration is estimated to be only $\pm 0.005 \text{ cm}^{-1}$. It should be noted that in this method of internal calibration any wave number shifts of the type mentioned in the last section are automatically allowed for.

C. Analysis of the $\beta(9,0)$ band

The $\beta(9,0)$ band is presented at the top of Fig. 2, and a portion of the spectrum is expanded below it to show the detail of rotational structure. We observed 117 lines and all lines are assigned to the six branches as listed in Table II. Most lines are separated, but a few blended lines are marked with a B following the wave numbers in the table. It is interesting to compare the results of Lagerqvist and Miescher²⁹ with the present results. We extended our observation to line as high as $J=23.5$, 20.5, 21.5, and 18.5 for the four major branches, R_{11} , P_{11} , R_{22} , and P_{22} in comparison with lines of J only 13.5, 14.5, 12.5, and 10.5, reported by Lagerqvist and Miescher. These differences, as well as those found in the R_{21} and Q_{11} branches, can be explained by the fact that Lagerqvist and Miescher²⁹ used low temperatures and high column densities.

The Λ -type doubling in the ground state of NO is well known³⁰ and is as small as 0.039 and 0.211 cm^{-1} at J

TABLE II. Observed wave numbers of the $\beta(9,0)$ band of NO.^a

J	$R_{11}(J)_e$	$R_{11}(J)_f$	$P_{11}(J)_e$	$P_{11}(J)_f$	$Q_{11}(J)$	$R_{22}(J)$	$P_{22}(J)$	$Q_{22}(J)$
0.5	54 186.393B				54 183.474			
1.5	54 186.393B		54 178.445		54 181.418	54 110.126		54 104.901
2.5	54 184.966		54 173.077b		54 177.986	54 108.820	54 096.300b	54 101.533
3.5	54 182.187		54 166.345b		54 173.216B	54 106.163	54 089.476	54 096.780b
4.5	54 178.053		54 158.220b			54 102.179	54 081.297	54 090.649
5.5	54 172.538b		54 148.737			54 096.742	54 071.766	54 083.242
6.5	54 165.634		54 137.925			54 089.971	54 060.919	54 074.384
7.5	54 157.415		54 125.709			54 081.829	54 048.593	54 064.169
8.5	54 147.889		54 112.129			54 072.382	54 034.964	54 052.654
9.5	54 136.984		54 097.230			54 061.401	54 019.982	
10.5	54 124.674	54 124.859	54 081.030			54 049.164	54 003.661	
11.5	54 111.010	54 111.213	54 063.425			54 035.523	53 985.816	
12.5	54 095.991	54 096.238b	54 044.417	54 044.610		54 020.493	53 966.751b	
13.5	54 079.611	54 079.845	54 024.094	54 024.304		54 004.066	53 946.287B	
14.5	54 061.883	54 062.113	54 002.384	54 002.620		53 986.272	53 924.393B	
15.5	54 042.754	54 043.009	53 979.305	53 979.559		53 967.105b	53 901.106B	
16.5	54 022.290	54 022.556	53 954.882	53 955.148		53 946.287B	53 876.435B	
17.5	54 000.444	54 000.738	53 929.072	53 929.358		53 924.393B	53 850.533b	
18.5	53 977.258	53 977.557	53 901.933	53 902.228		53 901.106B	53 823.031	
19.5	53 952.674	53 953.020	53 873.471	53 873.758		53 876.435B		
20.5	53 926.752	53 927.099	53 843.570	53 843.909		53 850.270b		
21.5	53 899.550	53 899.873				53 822.604		
22.5	53 870.879	53 871.176						
23.5	53 840.866	53 841.279						

Extra lines observed		
J	$R_{11}(J)$	$P_{11}(J)$
5.5	54 173.216b	
6.5	54 166.162b	
7.5	54 157.912b	54 126.425
8.5		54 112.590b
9.5		54 097.697

^aBlended lines followed by B are observed as a single line and by b are observed as an incompletely resolved complex.

=10.5 of ${}^2\Pi_{3/2}$ and ${}^2\Pi_{1/2}$, respectively. Lagerqvist and Miescher²⁹ did not observe the Λ -type doubling in their $\beta(9,0)$ band of NO. As shown in Table II, we have separated the Λ -type doubling in the $R_{11}(J)$ and $P_{11}(J)$ lines with $J \geq 10.5$ and 12.5, respectively. Some of these separations are also seen for the R_{11} branch lines in the bottom of Fig. 2. All the observed wave numbers were compared with those of Lagerqvist and Miescher,²⁹ and the differences in wave numbers are plotted in Fig. 3. Differences of the lines separated by Λ -type doubling were compared with those of the unseparated lines, and are presented by open circles and squares in the figure. We also noticed a few extra lines located close to the R_{11} and P_{11} lines with $J=5.5, 6.5,$ and $7.5,$ and $J=7.5, 8.5,$ and $9.5,$ respectively. They are listed in the bottom of Table II. We will discuss the extra lines later.

D. The rotational term values of the $B(9)$ level

The rotational term values of the $\nu=9$ level of the B ${}^2\Pi_r$ [$B(9)$] can be obtained by adding the term values of the $X(0)$ level to the wave numbers of the observed lines. The rotational term values of the $X(0)$ level relative to the level $\Omega = \frac{1}{2}, J=0.5, e$ are given by Amiot *et al.*³⁰ The averaged term values obtained from branch lines are listed in Table III with the estimated error bar. Only $F_1(J)$ levels with $J=11.5-24.5$ are obtained from the observation in the separate e and f components. We have assumed that the f

component has the higher energy, based on the separation in the ground state, but there is no internal evidence to back this assumption.

The effective Hamiltonian operator, suitable for the description of the ${}^2\Pi$ states, can be found in Hougen³¹ and Zare *et al.*³² The matrix elements used in this work for the

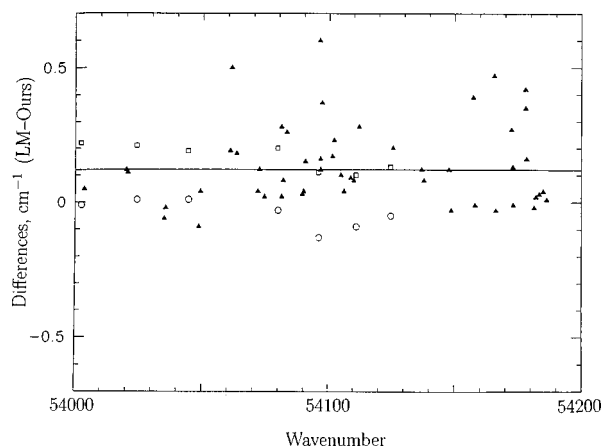


FIG. 3. Differences in the observed line positions between our results and Lagerqvist and Miescher (Ref. 29) are presented by solid triangles. Differences of the separated lines by Λ -type doubling are compared with those of the unseparated lines, and they are presented by open circles and squares. The solid horizontal line presents the averaged shifts of 0.12 cm^{-1} .

TABLE III. The term values and molecular constants of the $B(9) \ ^2\Pi$ level of NO, cm^{-1} .

J	$F_1(J), \ ^2\Pi_{1/2}$			$F_2(J), \ ^2\Pi_{3/2}$	
	e	f	<i>extra</i>	e	f
0.5	54 183.47±0.01	54 183.48±0.01			
1.5	54 186.42±0.02	54 186.44±0.02		54 229.80±0.03	54 229.81±0.03
2.5	54 191.40±0.01	54 191.43±0.02		54 235.04±0.01	54 235.04±0.01
3.5	54 198.33±0.01	54 198.38±0.01		54 242.33±0.01	54 242.33±0.01
4.5	54 207.26±0.01	54 207.30±0.01		54 251.71±0.01	54 251.71±0.01
5.5	54 218.15±0.01	54 218.23±0.01		54 263.21±0.02	54 263.21±0.02
6.5	54 231.02±0.02	54 231.10±0.01	54 231.75±0.05	54 276.68±0.01	54 276.68±0.01
7.5	54 245.85±0.01	54 245.94±0.01	54 246.39±0.07	54 292.26±0.01	54 292.27±0.01
8.5	54 262.71±0.01	54 262.80±0.01	54 263.24±0.06	54 309.92±0.02	54 309.92±0.02
9.5	54 281.60±0.01	54 281.71±0.02		54 329.68±0.01	54 329.69±0.01
10.5	54 302.45±0.01	54 302.57±0.01		54 351.35±0.01	54 351.35±0.01
11.5	54 325.25±0.01	54 325.57±0.02		54 375.20±0.01	54 375.21±0.01
12.5	54 350.06±0.02	54 350.40±0.05		54 401.06±0.03	54 401.06±0.03
13.5	54 376.80±0.01	54 377.20±0.05		54 428.94±0.02	54 428.96±0.02
14.5	54 405.54±0.02	54 405.95±0.01		54 458.86±0.02	54 458.87±0.02
15.5	54 436.27±0.02	54 436.71±0.01		54 490.83±0.03	54 490.85±0.03
16.5	54 468.96±0.02	54 469.41±0.01		54 524.85±0.02	54 524.87±0.02
17.5	54 503.65±0.02	54 504.12±0.01		54 560.77±0.02	54 560.80±0.02
18.5	54 540.32±0.01	54 540.80±0.01		54 598.71±0.02	54 598.74±0.02
19.5	54 578.95±0.02	54 579.46±0.01		54 638.82±0.02	54 638.85±0.02
20.5	54 619.53±0.02	54 620.08±0.02		54 680.95±0.03	54 680.98±0.03
21.5	54 662.11±0.02	54 662.67±0.02		54 725.00±0.03	54 725.03±0.03
22.5	54 706.72	54 707.30		54 770.92	
23.5	54 753.25	54 753.76			
24.5	54 801.74	54 802.37			
T_0	54 205.097	±0.012			
A	45.320	±0.021			
B_v	1.016 72	±0.000 16			
$D_v, 10^{-6}$	10.61	±0.32			
A_D	0.001 22	±0.000 11			

calculation of rotational energy levels are the same as those in Amiot *et al.*³³ and Stark *et al.*³⁴ The parameters included in the description of the $^2\Pi$ state are: The band origin T_0 ; the rotational parameters B , and D ; the spin-orbit parameters A and A_D ; and the Λ -doubling parameters p and q . In our analysis, we have performed least-squares fittings to the rovibronic term values. The term values corresponding to J numbering around $J=6.5-9.5$ were not included in the fit because a small perturbation has been detected. Table III summarized the molecular constants obtained for the $v=9$ level of the $B \ ^2\Pi$ state.

E. The rotational and band oscillator strengths of the $\beta(9,0)$ band

As mentioned in Sec. III A, the absorption lines are fitted to Voigt profiles while the Gaussian contribution is kept constant as 0.175 cm^{-1} . The fitting procedure provides integrated cross sections as well as line positions. These are independent of the anomalous widths, provided that the residuals from the fit are down at the noise level. The results of the integrated cross sections of lines are presented in Table IV. For blended lines the integrated cross sections have been separated by using branching ratios observed for other transitions together with the Boltzmann population distribution. The integrated cross sections of R_{11} branch lines are plotted in Fig. 4. The lines with $J>10$ consists of two lines e and f

components, indicated by open triangles and circles, respectively. The perturbed lines with $J=5.5-7.5$ give the extra lines and are shown by crosses. The total cross sections are presented by the solid squares. The cross sections are derived from the total column density of NO. Therefore, the integrated cross sections of lines depend on temperature, which was 295 K. The values listed in Table IV can be divided by the fractional population of the rotational level to obtain values proportional to the line oscillator strengths. The strengths of the branches are obtained by adding the integrated cross sections of all rotational lines in the branch. These are listed at the bottom line of Table IV.

The errors for the integrated cross sections can be obtained from the noise level, which in FT spectroscopy is virtually constant throughout the spectrum. Typically this translates into an uncertainty for a single point in the cross section of $\pm 4 \times 10^{-19} \text{ cm}^2$ (see Fig. 3) for lines that are on the linear part of the curve of growth; the uncertainty for partly saturated lines is rather greater. The standard deviation for a strong unblended line of integrated cross section $5 \times 10^{-18} \text{ cm}^2 \text{ cm}^{-1}$ is 4.5%. A conservative allowance for the small random error in pressure, temperature, and path length gives a maximum random error of $\pm 5\%$. For weak lines, the spectral noise dominates all other contributions, and the error on a single line may rise to $\pm 10\%$. Errors in the band oscillator strengths obtained by integration over all lines in the

TABLE IV. Integrated cross sections of lines of the $\beta(9,0)$ band of NO in units of $10^{-18} \text{ cm}^2 \text{ cm}^{-1}$.^a

J	$R_{11}(J)$			$P_{11}(J)$			$Q_{11}(J)$	$R_{22}(J)$ <i>e, f</i>	$P_{22}(J)$ <i>e, f</i>	$Q_{22}(J)$	
	<i>e</i>	<i>f</i>	<i>ext.</i>	<i>e</i>	<i>f</i>	<i>ext.</i>					
0.5	1.37B						1.07				
1.5	2.56B			1.55			0.40	1.56		1.95	
2.5	3.57			3.09b			0.00	2.27	1.47b	2.03	
3.5	3.99			4.70b				2.54	2.33	0.81b	
4.5	4.72			4.35b				3.55	2.30	0.68	
5.5	4.76b			5.22				3.42	2.55	0.56	
6.5	4.77			4.81				3.01	3.62	0.43	
7.5	4.19			3.82			0.43	3.40	2.83	0.18	
8.5	4.31			4.43			0.51b	4.08	2.92	0.13	
9.5	5.36			3.64			1.14	3.50	3.02		
10.5	4.27	1.05		5.25				2.48	3.93		
11.5	4.06	0.90		5.17				2.27	3.04		
12.5	3.41	0.76b		3.43	0.87			1.87	2.66b		
13.5	3.26	0.67		3.45	0.46			1.56	2.60B		
14.5	1.85	0.71		2.88	0.55			1.40	1.98B		
15.5	1.99	0.64		2.20	0.65			1.00b	1.67B		
16.5	1.67	0.54		1.89	0.49			0.84B	1.57B		
17.5	1.18	0.53		1.04	0.64			0.57B	1.22b		
18.5	0.93	0.39		0.97	0.39			0.41B	0.82		
19.5	0.63	0.37		1.26	0.14			0.46B			
20.5	0.54	0.27		0.65	0.17			0.25b			
21.5	0.67	0.08						0.13			
22.5	0.24	0.27									
23.5	0.15	0.11									
Total	74.55			70.24			1.47	40.57	40.76	6.75	

^aBlended lines followed by B are observed as a single line and by b are observed as an incompletely resolved complex.

band are dominated by the errors of the strong lines and are estimated to be about 5%.

The band oscillator strengths are given by

$$f(\nu', \nu'') = \frac{mc^2}{\pi e^2} \frac{1}{\tilde{N}(\nu'')} \int \sigma(\nu) d\nu, \quad (1)$$

in which $\tilde{N}(\nu'')$ is the Boltzmann population of the absorbing vibrational level, and the integration of the cross section $\sigma(\nu)$

is performed over all of the rotational lines belonging to the (ν', ν'') band. The integration of the cross sections of all observed rotational lines is equal to the summation of the integrated cross sections of all observed lines in Table IV, and it is $2.34 \times 10^{-16} \text{ cm}^2 \text{ cm}^{-1}$. The band oscillator strengths, $f(9,0)$, of the β band determined from the above integrated cross section is 2.65×10^{-4} . This value can be compared with previous published values of 3.14×10^{-4} by Chan *et al.*,³⁵ 3.7×10^{-4} by Cieslik,³⁶ and 3.58×10^{-4} by Bethke.¹⁷ Our value is the smallest, but is the only measurement to be done by a line by line measurement with a resolution comparable with the Doppler widths. Because Chan *et al.* could not separate the the $\beta(9,0)$ band from the $\delta(1,0)$ and the $\epsilon(0,0)$ band, it is possible that their blended measurements led to an over estimate of the band oscillator strength.

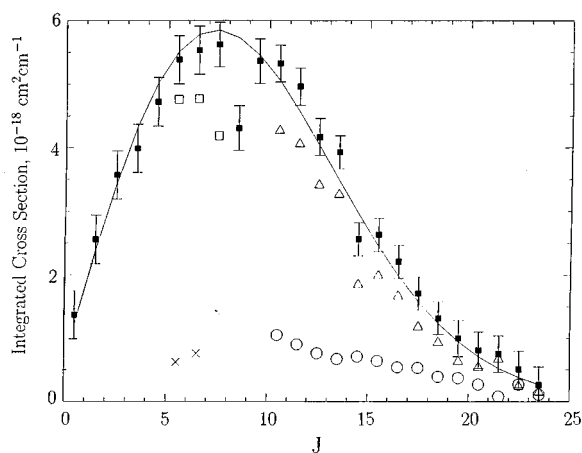


FIG. 4. The integrated cross sections of the R_{11} branch lines. The lines with $J > 10$ consists of two lines, *e* and *f* components, listed by open triangles and circles, respectively. For the perturbed lines with $J = 5.5$ – 7.5 , the main lines are shown in the open squares, and the extra lines are marked by crosses. The total cross sections are presented by solid squares with error bars mostly from static error of FT measurements.

IV. SUMMARY

This work provides the first absorption measurements of the $\beta(9,0)$ band of NO free of problems arising from inadequate spectral resolution. It is also the first report of absorption measurements of the NO bands performed by the combination of a VUV FT spectrometer and a synchrotron radiation source. The measurements obtained for the other NO bands summarized in Table I will be reported on later. Discussion of the perturbation in the vibronic levels and the band oscillator strengths will be given after the entire analyses of the NO bands is completed.

ACKNOWLEDGMENTS

This work was supported in part by a NSF Division of Atmospheric Sciences Grant No. ATM-94-22854 to Harvard College Observatory, and by the NASA Upper Atmospheric Research Program under Grant No. NAG5-484 to the Smithsonian Astrophysical Observatory. We also acknowledge the Paul Instrument Fund of the Royal Society for the development of the VUV-FT spectrometer. The FTS measurements at the Photon Factory were made with the approval of the Photon Factory Advisory Committee (94G367). K.Y. thanks the Japan Society for the Promotion of Science for support.

- ¹G. Brasseur and S. Solomon, *Aeronomy of the Middle Atmosphere* (Reidel, New York, 1984).
- ²T. Shimazaki, *Minor Constituents in the Middle Atmosphere* (Terra Scientific, Tokyo, 1985).
- ³M. Nicolet, *Ann. Geophys. (France)* **1**, 493 (1983).
- ⁴J. E. Frederick, A. J. Blake, and D. E. Freeman, *Handbook for MAP 8* (53 ICSC Scientific Committee on Solar Terrestrial Physics, Urbana, IL., 1983).
- ⁵K. P. Huber and G. Herzberg, *Molecular Spectra and Molecular Structure IV* (Van Nostrand Reinhold, New York, 1979).
- ⁶E. Miescher and K. P. Huber, *Spectroscopy*, edited by D. A. Ramsay (Butterworths, London, 1976).
- ⁷K. Yoshino, D. E. Freeman, J. R. Esmond, and W. H. Parkinson, *Planet. Space Sci.* **31**, 339 (1983).
- ⁸K. Yoshino, D. E. Freeman, J. R. Esmond, and W. H. Parkinson, *Planet. Space Sci.* **35**, 1067 (1987).
- ⁹K. Yoshino, J. R. Esmond, A. S.-C. Cheung, D. E. Freeman, and W. H. Parkinson, *J. Geophys. Res.* **95**, 11,743 (1990).
- ¹⁰S. Cieslik and M. Nicolet, *Planet. Space Sci.* **21**, 925 (1973).
- ¹¹J. E. Frederick and R. D. Hudson, *J. Atmos. Sci.* **36**, 737 (1979).
- ¹²M. Nicolet and S. Cieslik, *Planet. Space Sci.* **28**, 105 (1980).
- ¹³M. Allen and J. E. Frederick, *J. Atmos. Sci.* **39**, 2066 (1982).
- ¹⁴K. Minschwaner and D. E. Siskind, *J. Geophys. Res.* **98**, 20,401 (1993).
- ¹⁵D. J. Hart and O. L. Bourne, *Chem. Phys.* **133**, 103 (1989).
- ¹⁶J. E. Murray, K. Yoshino, J. R. Esmond, W. H. Parkinson, Y. Sun, A. Dalgarno, A. P. Thorne, and G. Cox, *J. Chem. Phys.* **101**, 62 (1994).
- ¹⁷G. W. Bethke, *J. Chem. Phys.* **31**, 662 (1959).
- ¹⁸S. Cieslik, *Bull. Cl. Sci. Acad. R. Belg.* **63**, 884 (1977).
- ¹⁹J. A. Guest and L. C. Lee, *J. Phys. B* **14**, 3401 (1981).
- ²⁰R. D. Hudson, *Rev. Geophys. Space Phys.* **9**, 305 (1971).
- ²¹W. H. Parkinson, A. P. Thorne, G. Cox, P. L. Smith, and K. Yoshino, *Ultraviolet Technology V, Proc. (SPIE 2282)*, 1994).
- ²²A. P. Thorne, C. J. Harris, I. Wynne-Jones, R. C. M. Learner, and G. Cox, *J. Phys. E: Sci. Instrum.* **20**, 54 (1987).
- ²³K. Ito, Y. Morioka, T. Sasaki, H. Noda, K. Goto, T. Katayama, and M. Koike, *Appl. Opt.* **25**, 837 (1986).
- ²⁴J. W. Brault (private communication).
- ²⁵P. M. Dooley, B. R. Lewis, S. T. Gibson, G. H. Baldwin, P. C. Cosby, J. L. Price, R. A. Copeland, T. G. Slinger, K. Yoshino, A. P. Thorne, and J. E. Murray, *J. Chem. Phys.* (to be published).
- ²⁶K. Yoshino, J. E. Murray, J. R. Esmond, Y. Sun, and W. H. Parkinson, A. P. Thorne, R. C. M. Learner, and G. Cox, *Can. J. Phys.* **72**, 1101 (1994).
- ²⁷V. Kaufman, *J. Opt. Soc. Am.* **52**, 866 (1962).
- ²⁸D. Lecler, *C. R. Acad. Sci. Paris*, **266B**, 1509 (1968).
- ²⁹A. Lagerqvist and E. Miescher, *Helv. Phys. Acta* **31**, 221 (1958).
- ³⁰C. Amiot, R. Bacis, and G. Guelachvili, *Can. J. Phys.* **56**, 251 (1978).
- ³¹J. T. Hougen, *NBS Monograph 115* (Washington, DC., 1970).
- ³²R. N. Zare, A. L. Schmeltekopf, D. L. Albritton, and W. J. Harrop, *J. Mol. Spectrosc.* **48**, 174 (1973).
- ³³C. Amiot, J.-P. Maillard, and J. Chauville, *J. Mol. Spectrosc.* **87**, 196 (1981).
- ³⁴G. Stark, J. W. Brault, and M. C. Abrams, *J. Opt. Soc. Am. B* **11**, 3 (1994).
- ³⁵W. F. Chan, G. Cooper, and C. E. Brion, *Chem. Phys.* **170**, 111 (1993).
- ³⁶S. Cieslik, *Bull. Cl. Sci. Acad. Roy. Belg.* **63**, 884 (1977).